https://doi.org/10.5194/egusphere-2026-55
Preprint. Discussion started: 15 January 2026

A coupled surface water-groundwater multi-objective optimization framework for coordinated water-ecosystem-agriculture management in arid inland river basin

Danhong Chen[1], Xiankui Zeng[1] *, Dongwei Gui[2], Dong Wang[1], Jichun Wu[1]

[1]Key Laboratory of Surficial Geochemistry, Ministry of Education, School of Earth Sciences and Engineering, Nanjing University, Nanjing, China

[2]Cele National Station of Observation and Research for Desert-Grassland Ecosystem, Xinjiang Institute of Ecology and Geography, Chinese Academy of Sciences, Urumqi, China

Correspondence to: Xiankui Zeng (xiankuizeng@nju.edu.cn)

Abstract: In arid regions, water is the key link sustaining both production and ecosystems, and its sustainable management is essential for regional security. This study constructs a coupled surface water-groundwater hydrology-agriculture multi-objective optimization model for the mainstream area of the Tarim River Basin, in which the NSGA-III algorithm is applied to optimize four objectives, including agricultural economic benefit per unit of irrigation water (f_{AB}), groundwater level rise (f_{GL}), terminal lake area (f_{LA}), and total agricultural nitrogen load (f_{TN}). Based on the optimized solutions, the trade-offs and synergistic pathways among multiple objectives within the water-ecosystem-agriculture system are systematically evaluated under different hydrological year conditions. The results indicate that significant trade-offs exist among objectives, with f_{AB} showing negative relationships with f_{TN} and f_{LA}, and solutions with higher economic benefits generally accompanied by reduced ecological water supply and increased nitrogen loads. The spatial heterogeneity of the basin necessitates the adoption of differentiated management strategies, whereby upstream areas with relatively stable water availability can sustain higher levels of agricultural production, while midstream and downstream areas are highly sensitive to ecological water constraints and therefore require priority allocation to ecological water use. The optimization results show that cultivated land area should be dynamically adjusted under different hydrological conditions, ranging from 11.3-14.3×10⁴ hm^2 in wet years, 10.1-13.1×10⁴ hm^2 in normal years, and contracting to 9.5-11.9×10⁴ hm^2 in dry years. The cropping structure is dominated by cotton (69.7%-75.8%), with the proportion of high-benefit crops such as vegetables and fruit crops moderately increased in wet years, whereas in dry years the structure shifts toward water-saving crops and high water-consuming crops are appropriately restricted. This study demonstrates that combining multi-objective optimization with spatially differentiated regulation can achieve coordinated management of water resources, ecosystems, and agriculture, and provides an operational decision-making basis for managing water-ecosystem-agriculture systems in arid inland river basins.

Keywords: Surface water-groundwater; Multi-objective optimization; Hydrological model; Arid river basin

https://doi.org/10.5194/egusphere-2026-55
Preprint. Discussion started: 15 January 2026

1 Introduction

The continuous growth of the global population and the expansion of cultivated areas have exacerbated the imbalance between water availability and demand, with particularly severe impacts in arid and semi-arid regions (IPCC, 2022; Flörke et al., 2018; Cosgrove and Loucks, 2015; Watson et al., 2013). Agriculture is responsible for nearly 70% of global freshwater withdrawals (FAO, 2012) and contributes nearly 25% of global greenhouse gas emissions (Campbell et al., 2017). Under the combined pressures of water scarcity and ecosystem vulnerability, improving the understanding of interactions within the water-ecosystem-agriculture (WEA) system and developing coordinated multi-objective optimization frameworks have become critical for achieving sustainable water resources management (Yin et al., 2022; Song et al., 2020; Jalilov et al., 2018; Avellán et al., 2018).

In recent years, multi-objective simulation optimization (S-O) frameworks have been increasingly applied to basin-scale water resources management and planning. By coupling process-based simulation models with multi-objective optimization algorithms, these frameworks provide an effective means of exploring trade-offs among water allocation, ecosystem protection, and agricultural production within the WEA system (Song et al., 2020; Niu et al., 2019; Karner et al., 2021; Wang et al., 2022; Cao et al., 2023; Naranjo et al., 2023). For instance, Niu et al. (2019) employed a multi-objective linear fractional programming model to assess the interactions and trade-offs among water resources, ecosystems, and agriculture activities in the Zhangye Basin. Yin et al. (2022) coupled a SEAWAT-RT3D model with multi-objective optimization to quantify trade-offs between agricultural net benefits, seawater intrusion, and nitrate contamination in the Dagu River Basin. Similarly, Zhang and Ren (2021) and Tang et al. (2024) applied S-O frameworks in the Haihe River Basin and the Yanqi Basin, respectively, and achieved coordinated improvements in economic and ecological outcomes under regulated water allocation scenarios. These studies demonstrate the applicability and effectiveness of S-O frameworks for addressing WEA trade-offs at the regional scale.

The mainstream reach of the Tarim River Basin represents a representative arid inland river system in China. Agricultural production in this region is highly dependent on hydraulic infrastructure and is characterized by intensive irrigated agriculture. Long-term and large-scale abstraction of groundwater and diversion of surface water for irrigation have supported regional agricultural development and food security. However, these practices have also resulted in pronounced ecosystem degradation, manifested by declining groundwater levels, intensified desertification, and the shrinkage of terminal lakes. Consequently, the need to balance agricultural water use with ecosystem stability has become a critical concern for the oversight of water resources in the Tarim River Basin.

In response to these challenges, numerous studies have investigated agricultural irrigation efficiency, ecological water allocation, and optimal water resources management in the basin. Chen (2018) developed a bi-objective optimization model to analyze benefit allocation between agricultural and ecological water uses under different inflow scenarios. Jia (2020) proposed an ecological water-use priority system and ecological replenishment strategies based on eco-gate control zones.

https://doi.org/10.5194/egusphere-2026-55
Preprint. Discussion started: 15 January 2026

Zhu (2022) established a regional water allocation optimization model to support the coordinated operation of multiple water sources. From a water-energy-food (WEF) nexus perspective, Feng et al. (2023) assessed the irrigation requirements and overall efficiency of resource utilization for the main crops in the basin.

Despite these advances, existing studies still exhibit limitations in their representation of the physical mechanisms and coordinated management of the WEA system. Many studies rely on simplified modeling approaches that treat surface water and groundwater as separate components, thereby failing to capture their dynamic interactions. This limitation constrains the accurate quantification of the impacts of land-use change or cropping structure adjustment on groundwater dynamics and ecosystem responses. In addition, ecological water requirements are often represented as fixed minimum thresholds, which overlook the dynamic regulatory role of surface water-groundwater interactions over time. As a result, ecological constraints are not effectively incorporated into optimization-based decision-making processes. Moreover, most existing studies focus on single or dual objectives, such as agriculture-ecology or agriculture-economy, and lack a comprehensive optimization framework that systematically characterizes trade-offs among water resources, ecosystems, and agriculture within the WEA system.

To address these limitations, this study develops a WEA collaborative optimization framework for the mainstream reach of the Tarim River Basin by integrating a coupled surface water-groundwater model, multi-objective optimization, and dynamic ecological constraints. The objectives of this study are twofold. First, a multi-objective S-O model incorporating surface water-groundwater interactions is constructed to achieve coordinated optimization of water resources, ecosystems, and agriculture within the WEA system of the Tarim River mainstream region. Second, based on the proposed WEA optimization framework, critical thresholds of cultivated land expansion and optimal cropping structures under different hydrological conditions are identified. This study aims to provide scientific support for sustainable water resources management in arid inland river basins.

The remainder of this paper is organized as follows. Section 2 describes the study area and data sources. Section 3 details the adopted modeling approach, covering the coupled surface water-groundwater simulation, the multi-objective optimization method, and the evaluation metrics. Section 4 reports the simulation and optimization results. Section 5 provides a discussion of the results and their implications, while Section 6 summarizes the main conclusions and outlines future research directions.

2. Study area and data

2.1 Study area

The mainstream region of the Tarim River Basin is situated in northern Xinjiang, China, between the southern alluvial plain of the Tianshan Mountains and the northern margin of the Taklimakan Desert. The study region stretches westward from the Alar region, where the Aksu, Yarkant, and Hotan rivers merge, eastward to the terminal Taitema Lake (Fig. 1).

https://doi.org/10.5194/egusphere-2026-55
Preprint. Discussion started: 15 January 2026

The study area covers approximately 40,956 km², featuring a gently eastward-sloping topography with elevations ranging from 805 to 1023 m.

The region exhibits a temperate continental arid climate, characterized by an annual mean temperature of 10.6 °C and total precipitation below 80 mm, mainly occurring from May to August, while the annual potential evapotranspiration is over 2500 mm. Water resources primarily originate from mountain glacier/snowmelt and upstream inflow diversions, exhibiting the arid-region characteristics of source-dominated supply with high spatiotemporal variability.

The Tarim River mainstream stretches approximately 1321 km in a west-east direction and is typically categorized into upstream, midstream, and downstream sections. The river exhibits a strongly seasonal flow pattern, with 70%-85% of the annual runoff occurring from June and September. Peak flows usually occur in July or August, whereas minimum flows are typically recorded in January and February. Surface water and groundwater systems within the region are closely connected, with frequent interactions influencing regional water availability.

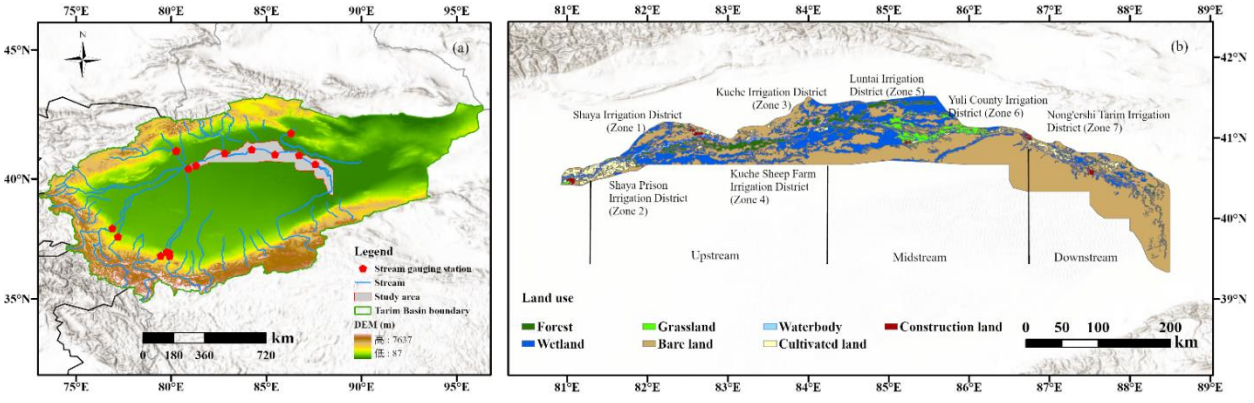

Figure 1. (a) The location of the Tarim River mainstream region. (b) Land use types across the Tarim River mainstream region. Sources: Esri; Powered by Esri; Basemap: Esri World 286 Hillshade (Esri).

Agriculture is the dominant economic activity in the Tarim River mainstream region. By 2015, approximately 1307 km² of land were under irrigation, of which about 1073 km² is cultivated land. Major crops include cotton, maize, vegetables, and fruits. Since 1990, the cultivated land area has expanded by over 60%, with oasis farmland continually encroaching into desert margins.

The area contains several large irrigation districts, where water for irrigation is primarily drawn from the Tarim River mainstream, supplemented by groundwater. Considerable differences in management and irrigation efficiency among these districts have placed significant pressure on the distribution of mainstream water resources, complicating regional water management.

https://doi.org/10.5194/egusphere-2026-55
Preprint. Discussion started: 15 January 2026

The downstream ecosystem is extremely fragile. Ecological degradation has intensified since the 1950s with the area of Populus euphratica forests decreasing by approximately 86% compared to historical conditions. The river reaches between Daxihaizi Reservoir and Taitema Lake experienced prolonged channel desiccation, including a continuous dry-up of nearly 400 km at its most severe stage. As a result, Taitema Lake remained dry for extended periods, and the margins of the Taklimakan and Kuruk deserts approached near connection.

To mitigate ecological degradation in downstream reaches, China launched the Ecological Water Conveyance Project (EWCP) along the Tarim River mainstream in 2000, aiming to restore river connectivity, groundwater levels, and riparian vegetation in downstream areas. According to recent monitoring and official reports, 26 ecological water conveyance events had been conducted by 2025, delivering a cumulative volume of approximately 10.2 billion m^3.

The ecological water conveyance has substantially improved riparian vegetation coverage, wetland area, and groundwater levels along the downstream river corridor, playing a critical role in the recovery of ecosystem functions (Liao et al., 2020).

Despite these improvements, continued agricultural expansion upstream has increased diversion demands, while interannual inflow variability further strains ecological water regulation. Consequently, there remains a need to further optimize mainstream water resources allocation, improve irrigation water use efficiency, and achieve a dynamic balance between ecological water conveyance and agricultural development, in order to safeguard basin-wide ecological security and socio-economic sustainability.

2.2 Data

The datasets used in this research encompass topography, land use, climate, hydrogeology, and socio-economic information, with a primary temporal coverage from 2002 to 2021. The data sources and corresponding processing methods are described in detail below.

Snow cover information was obtained from the High Asia MODIS daily snow cover fraction product developed by Qiu and Wang (2020). This dataset , derived using the MODIS Normalized Difference Snow Index (NDSI), offers daily data at a spatial resolution of 500 m and serves as a critical inputs for the snowmelt runoff model (SRM). Terrain-related information was sourced from the Advanced Spaceborne Thermal Emission and Reflection Radiometer Global Digital Elevation Model (ASTER GDEM), which has a spatial resolution of 30 m (NASA/METI, 2019). These elevation data were used to extract terrain attributes, including slope, aspect, and river networks.

Land use, vegetation, and soil property data were obtained from multiple sources. Land cover information was obtained from the FROM-GLC dataset (Gong et al., 2013), soil properties were derived from the Harmonized World Soil Database (Wieder et al., 2014), and vegetation attributes were derived from the Vegetation Map of China (Li et al., 2017). Collectively,

https://doi.org/10.5194/egusphere-2026-55
Preprint. Discussion started: 15 January 2026

these datasets provided key inputs for simulating land surface processes and parameterizing soil-related processes in the coupled model.

Hydrogeological conditions were primarily derived from borehole data and regional hydrogeological maps reported by Li et al. (2003). These data were used to delineate aquifer lithology and structural features across plain and desert environments. Key parameters, such as hydraulic conductivity and effective porosity, were assigned according to dominant lithological units and parameter ranges reported in previous studies.

Meteorological forcing for the coupled surface water-groundwater model consisted of precipitation and temperature (maximum and minimum), which were obtained from the ERA5 reanalysis dataset (Hersbach et al., 2020). Model calibration and validation for the groundwater component relied on monthly groundwater level measurements from 139 monitoring wells distributed throughout the study area (Xue et al., 2024).

Daily streamflow records from eight representative hydrological stations within the Tarim River Basin were also used. These records cover the period from 2002 to 2021 and were employed to calibrate surface runoff simulations and associated model parameters.

To further evaluate the GSFLOW model, terrestrial water storage anomaly (TWSA) data from the GRACE and GRACE-FO satellite missions were incorporated. The analysis employed the RL06 Mascon Level-3 product released by the Center for Space Research at the University of Texas at Austin (Save et al., 2016; Save, 2024), covering April 2002 through December 2021. Missing monthly records were reconstructed using cubic spline interpolation, while data gaps between the GRACE and GRACE-FO missions were filled using reconstructed terrestrial water storage datasets developed by Zhong et al. (2019, 2020).

Monthly terrestrial water storage change (TWSC) was calculated from the TWSA series as follows:

$$TWSC(t) = TWSA(t) - TWSA(t-1) \quad (1)$$

where TWSC(t) represents the change in terrestrial water storage(mm) during month t, and TWSA(t) represents the corresponding storage anomaly.

Beyond streamflow and GRACE-based evaluations, additional validation of the coupled model was conducted using independent datasets that describe evapotranspiration and soil moisture dynamics. Evapotranspiration data were obtained from the GLEAM v3.6a product (Martens et al., 2017) and compared with simulated regional values. Soil moisture observations were taken from the Chinese Soil Moisture Dataset (Mao, 2021; Meng et al., 2021) to evaluate the temporal behavior of simulated soil moisture.

Socio-economic data were primarily collected from the China Statistical Yearbook (National Bureau of Statistics, 2002-2021), Xinjiang Water Resources Bulletin (Xinjiang Water Resources Department, 2002-2021), and the National

https://doi.org/10.5194/egusphere-2026-55
Preprint. Discussion started: 15 January 2026

Agricultural Product Cost-Benefit Compilation together with annual crop price statistics (Ministry of Agriculture and Rural Affairs of Xinjiang, 2002-2025). These datasets provide information on crop planting areas, yields, and fertilizer and pesticide application rates. A comprehensive summary of all datasets employed in this study is provided in Table 1.

Table 1. Data for the coupled hydrology-agriculture optimization framework.

Data	Dataset / Source	Spatial & Temporal Resolution	Usage
Snow cover	High Asia MODIS daily snow cover fraction dataset	500 m| Daily	Model input
Climate forcing	ERA5 reanalysis	0.25°×0.25°| hourly	Model input
Topography	ASTER GDEM	30 m	Model input
Hydrogeology	hydrogeological maps, borehole data	Site-specific	Model input
Land surface	FROM-GLC, HWSD. Vegetation Map of China,	Dataset-specific	Model input
Socio-economic data	XSB, XWRB, NAPCBC & ARAX	Annual	Model input
Groundwater level	Monitoring wells	Monthly	Model validation
Terrestrial water storage changes	GRACE/GRACE-FO (CSR RL06 Mascon)	0.25°×0.25°| month	Model validation
Evapotranspiration	GLEAM	0.25°×0.25°|monthly	Model validation
Soil moist	Soil Moisture in China dataset	0.05°×0.05°|monthly	Model validation

3. Methodology

This study develops a comprehensive decision-oriented framework that combines a coupled surface water-groundwater simulation with a multi-objective optimization approach. The framework is designed to simulate hydrological processes within the Tarim River mainstream region and to achieve coordinated optimization of agricultural and ecological water demands under limited water availability. The overall modeling system consists of three components. The first component is a GSFLOW-based hydrological model that simulates interactions between surface water and groundwater. The second component is a snowmelt runoff model (SRM), which captures snow and glacier melt processes occurring in the mountainous headwater areas of the basin. The third component is a multi-objective water-ecosystem-agriculture (WEA) optimization model, which is applied to coordinate water allocation among water resources, ecosystems, and agricultural production.

3.1 Coupled hydrological simulation

Although the primary focus of this study is the Tarim River mainstream region, accurate representation of surface water-groundwater exchanges necessitates hydrological simulations at the scale of the entire Tarim River Basin. The

https://doi.org/10.5194/egusphere-2026-55
Preprint. Discussion started: 15 January 2026

hydrological simulation framework consists of the SRM and the GSFLOW model. The SRM is applied to simulate snow and glacier melt runoff at the mountain outlets, and the simulated results are subsequently used as the upstream inflow boundary for the GSFLOW model. GSFLOW model is then employed to simulate hydrological processes across the Tarim River plain and downstream desert areas. The basin-scale simulation outputs are then used to extract boundary conditions and fluxes for the mainstream region, which serves as the domain for the subsequent multi-objective WEA optimization.

3.1.1 Coupled surface water-groundwater model

The coupled surface water-groundwater model is developed based on the GSFLOW framework proposed by Chen et al. (2025), with model parameters recalibrated in this study. Specifically, we incorporated additional streamflow observations from three mainstream stations (Yingbazha, Usman, and Qiala) to refine parameter estimation. Diversion flows from major mainstream irrigation canals were also adjusted during calibration.

The model integrates the PRMS surface hydrology module with the MODFLOW-NWT groundwater flow module to simulate hydrological processes from precipitation through the subsurface system. The modeling domain encompasses the Tarim River plain and surrounding desert areas and is discretized at a spatial resolution of 2 km×2 km, yielding a total of 212,928 hydrologic response units (HRUs). The groundwater system is discretized into six layers, comprising 692,658 active grid cells.

Surface processes (infiltration, evapotranspiration, irrigation recharge) are parameterized based on geomorphology, land use, and crop distribution. Irrigation infiltration and groundwater abstraction volumes are derived from the Xinjiang Water Resources Bulletin (2002-2021). Other key parameters (e.g., infiltration coefficients, aquifer hydraulic conductivity) were calibrated using a Bayesian uncertainty analysis framework.

The simulation period spans 2002-2021, with 2002-2006 designated as the warm-up period, 2007-2016 as the calibration period, and 2017-2021 as the validation period. Model calibration and validation are conducted using observed groundwater levels and streamflow data from major hydrological stations. Additional evaluation of the calibrated GSFLOW model is conducted using GRACE-based terrestrial water storage change (TWSC), evapotranspiration data from the GLEAM product, and soil moisture data from the SMC dataset.

Model performance is quantified using the Nash-Sutcliffe efficiency (NSE) and the coefficient of determination (R^2), defined as follows:

$$\mathrm{NSE} = 1 - \frac{\sum_{i=1}^{n}\left(Q_{sim}(i) - Q_{obs}(i)\right)^2}{\sum_{i=1}^{n}\left(Q_{obs}(i) - \overline{Q_{obs}}\right)^2} \tag{2}$$

$$R^2 = \frac{\left[\sum_{i=1}^{n}\left(Q_{obs}(i) - Q_{obs}(i)\right)\left(Q_{sim}(i) - \overline{Q_{sim}}(i)\right)\right]^2}{\left[\sum_{i=1}^{n}\left(Q_{obs}(i) - \overline{Q_{obs}}\right)^2\right]\left[\sum_{i=1}^{n}\left(Q_{sim}(i) - \overline{Q_{sim}}\right)^2\right]} \tag{3}$$

https://doi.org/10.5194/egusphere-2026-55
Preprint. Discussion started: 15 January 2026

where n is the length of the observation series; $Q_{obs}(i)$ and $Q_{sim}(i)$ denote the observed and simulated values at time step i, respectively; and Q_{obs} and Q_{sim} represent their corresponding mean values. Both NSE and R^2 range from 0 to 1, with values approaching 1 indicating stronger agreement between simulations and observations.

3.1.2 Snowmelt runoff model (SRM)

Snow and glacier melt from mountainous regions represent a critical source of water supply in the Tarim River Basin. To account for these processes, the SRM model is applied to simulate daily snowmelt runoff. The model incorporates temperature, precipitation, and snow cover fraction, and is expressed as follows:

$$Q_{n+1}=[c_{sn}\cdot M_n\cdot S_n+c_{Rn}\cdot P_n]\cdot A\cdot\frac{10000}{86400}(1-k_{n+1})+Q_n\cdot k_{n+1} \quad (4)$$

where Q_{n+1} is the mean daily discharge on day n+1 (m^3/s); Mn and P_n are the snowmelt depth (cm/d) and precipitation (cm) on day n, respectively; S_n is the snow cover fraction; c_{sn} and c_{Rn} are the runoff coefficients for snowmelt and rainfall; A is the basin area (km^2); k_{n+1} is the recession coefficient representing runoff decay under no recharge conditions; and the factor 10000/86400 converts runoff depth (cm) to discharge (m^3/s).

3.2 Multi-objective optimization model

To promote the coordinated development of agricultural production, ecosystem protection, and sustainable water resources use, a multi-objective water-ecosystem-agriculture (WEA) optimization model was developed for the Tarim River Basin mainstream region. Based on regional geomorphological features and hydrological conditions, the mainstream area was initially categorized into three major sections: upstream, middle, and downstream reaches. Each section was further partitioned into seven agricultural management sub-units. This zoning scheme primarily follows administrative divisions in combination with the spatial distribution of major irrigation districts. The seven agricultural sub-units include the Shaya Irrigation District (Zone 1), Shaya Prison Irrigation District (Zone 2), Kuqa Irrigation District (Zone 3), Kuqa Sheep Breeding Farm Irrigation District (Zone 4), Luntai Irrigation District (Zone 5), Yuli County Irrigation District (Zone 6), and the Second Agricultural Division Tarim Irrigation District (Zone 7). The geographical arrangement of these sub-units is illustrated in Fig. 1(b).

3.2.1 Decision variables

The proposed multi-objective optimization model includes two categories of decision variables, namely crop planting areas and monthly ecological water allocation coefficients.

(1) Crop planting area (A_{ij})

For model implementation, the mainstream region is divided into multiple agricultural zones according to natural geographic attributes and administrative boundaries. Within each zone, multiple crop types are considered, including maize,

https://doi.org/10.5194/egusphere-2026-55
Preprint. Discussion started: 15 January 2026

cotton, vegetables, melons, fruit trees, and oilseeds. The variable A_{ij} denotes the cultivated area of crop j in agricultural zone i, expressed in units of thousand hectares.

(2) Monthly ecological water allocation coefficient (θ_k)

To represent the seasonal characteristics of ecological water demand, the period from May to September is identified as the key ecological water replenishment period. The coefficient θ_k represents the proportion of the annual total ecological water allocation assigned to month k.

3.2.2 Constraints

To ensure that the optimization process complies with regional hydrological conditions and ecological safety requirements, the following constraints are imposed.

(1) Groundwater depth constraint

The groundwater depth in each ecological zone is required to remain within a suitable range for vegetation growth and sustainability. This constraint is expressed as:

$$H_{min} \leqslant H_{s,t} \leq H_{max} \quad (5)$$

where $H_{s,t}$ denotes the groundwater depth in zone s at time t. Based on previous studies, the suitable groundwater depth ranges are 3-6 m for forestland, 2-5 m for grassland, and 4.5-7 m for desert vegetation (Wang et al., 2020).

(2) Terminal lake area constraint

The surface extent of Taitema Lake, as the terminal lake, is constrained to remain within a prescribed range in order to maintain its basic ecological functions. The constraint is defined as:

$$A_{min} \leq A \leq A_{max} \quad (6)$$

where A_{min} and A_{max} are set to 30 km² and 110 km², respectively. These values are derived from remote sensing observations over the past 30 years and studies on ecological water requirements, which indicate that this range is sufficient to sustain key ecosystem functions and biodiversity within the lake system (Ye et al., 2022; Wang et al., 2021).

(3) Canal conveyance capacity constraint

The diversion flows allocated to agricultural and ecological zones must not exceed the conveyance capacity of the canal system. This constraint is formulated as:

$$Q_{a,i} \leq Q_{max,i} \quad (7)$$

$$Q_{e,j} \leq Q_{max,j} \quad (8)$$

https://doi.org/10.5194/egusphere-2026-55
Preprint. Discussion started: 15 January 2026

where $Q_{a,i}$ and $Q_{e,j}$ represent the diversion flows for agricultural zone i and ecological zone j ($m^3\ s^{-1}$), respectively. The maximum conveyance capacities Q_{max} are determined based on the design discharge and conveyance capacity of major canals along the mainstream (Wang et al., 2021).

(4) Crop water requirement

The effective irrigation water supplied to each agricultural zone must satisfy the basic water requirements of crops. This requirement is expressed as:

$$Q_{ai}\alpha\beta \geq \mathrm{I}_{ij} \tag{9}$$

where α and β denote the canal conveyance efficiency and field application efficiency, respectively, and I_{ij} represents the irrigation demand (mm) associated with crop *j* in agricultural zone *i*.

3.2.3 Objective functions

The multi-objective model targets the maximization of agricultural economic benefits, groundwater level recovery, and the surface area of the terminal lake, in parallel with the minimization of total nitrogen load.

(1) Maximize agricultural economic benefit per unit of irrigation water

$$Maximize\ f_{AB} = \sum_{i=1}^{K} P_i A_i Y_i - \sum_{i=1}^{K} \frac{C_i Q_{ai} A_i}{\lambda_i} \tag{10}$$

(2) Maximize average cumulative groundwater level rise

$$Maximize\ f_{GL} = \frac{1}{N}\sum_{i=1}^{N} H_{iT} - H_{i1} \tag{11}$$

(3) Maximize Taitema Lake surface area

$$Maximize\ f_{LA} = A_{area} \tag{12}$$

(4) Minimize total nitrogen load

$$Minimize\ f_{TN} = \sum_{i=1}^{K} N_i A_i \tag{13}$$

where P_i represents the unit net economic benefit of crop i (CNY/m^3); A_i denotes the irrigated area in agricultural zone i (hm^2); K represents the total count of agricultural zones,with $K = 7$; Y_i corresponds to the crop yield per unit area; C_i denotes the unit water cost (CNY/m^3); λ_i is the irrigation water use efficiency; T indicates the number of stress periods (T=365, d);N denotes the total number of grid cells across the study domain; H_{iT} and H_{i1} denote the groundwater heads at grid cell i at the last and first stress periods, respectively; A_{area} represents the surface area of Taitema Lake (km^2); $Q_{a,i}$ and $Q_{e,i}$ denote agricultural and ecological diversion volumes (m^3/month) , respectively; and N_i represents the total nitrogen load per unit

https://doi.org/10.5194/egusphere-2026-55
Preprint. Discussion started: 15 January 2026

area of crop i (kg/hm^2). Each irrigation district encompasses six crop types, which are maize, cotton, vegetables, melons, fruit crops, and other crops. The crop management parameters are summarized in Table 2.

Table 2. Parameters related to crop planting management.

Crop type	Market price (CNY/ kg)	Irrigation quotas (m^3/hm^2)	Cultivation cost (CNY/hm^2)	Total nitrogen loading (kg/hm^2)
Maize	2.0	5250	1463	339.7
Cotton	7.4	6750	1463	456.7
Vegetable	2.2	6750	1967	450.0
Cucurbits	3.6	5250	1967	350.0
Fruit	3.0	5250	1420	320.0
Oilseed	6.4	7350	1420	280.0

The above multi-objective optimization problem is addressed using the Non-dominated Sorting Genetic Algorithm III (NSGA-III; Deb and Jain, 2014). This algorithm is particularly effective for handling high-dimensional problems involving multiple objectives and constraints and has been extensively employed in studies of environmental and agricultural resource optimization. The main algorithm parameters are listed in Table 3.

Table 3. The parameters of the NSGA-III.

Parameter	Value
Population size (N_{pop})	300
Maximum number of generations (G_{max})	6000
Crossover probability (P_c)	0.9
Mutation probability (P_m)	0.05
Epsilon resolution	(1.0, 0.01, 0.001)

3.3 Surrogate model for basin-scale hydrological simulation

Each GSFLOW simulation takes approximately 18 hours, presenting a prohibitive computational cost for the simulation-optimization framework. To overcome this, a surrogate model was constructed using a radial basis function neural network (RBF-NN) to represent the relationship between key GSFLOW parameters and the four objective functions in the multi-objective optimization model. The RBF-NN is a multilayer feedforward network with strong nonlinear approximation capability and high computational efficiency. Training samples are generated using Latin hypercube sampling (LHS) to ensure adequate coverage of the parameter space. Following accuracy validation, this surrogate model replaces the original GSFLOW model within the simulation-optimization loop.

https://doi.org/10.5194/egusphere-2026-55
Preprint. Discussion started: 15 January 2026

4. Results

4.1 Calibration and validation of the basin-scale hydrological model with surrogate model assessment

Simulated daily runoff from the SRM model agrees well with observations, particularly during spring snowmelt, where both the timing and magnitude of peak flows are accurately captured. The SRM achieves Nash-Sutcliffe efficiency (NSE) values between 0.72 and 0.96, demonstrating its strong capability to accurately simulate seasonal snowmelt-driven runoff. These results demonstrate the SRM's capability in capturing the temporal variability of mountain inflows, making it suitable for providing reliable upstream boundary conditions to the GSFLOW model. The spatial distribution and numbering of the 22 sub-basins with available observations, as well as the corresponding SRM simulation results and comparisons with observed runoff, are shown in Fig. S1-S3 in the Supplementary Material.

As shown in Fig. 2, GSFLOW simulations closely match observed monthly streamflow at Alar, Xinqiman, Yingbaza, Wusiman, and Qiala stations on the Tarim River main stem, with NSE values ranging from 0.6 to 0.7. This demonstrates that the model adequately represents runoff dynamics, including both high- and low-flow periods.

Figure 3 depicts the agreement between observed and modeled groundwater levels at 139 monitoring wells throughout the validation period. The NSE of the groundwater simulation reached 0.96, demonstrating that the GSFLOW model can accurately capture groundwater dynamics at the observation points. It should be noted that the monitoring wells are unevenly distributed and limited in number, being mainly concentrated in the main stem of the Tarim River and the Hetian region.

The reliability of the GSFLOW model was further evaluated by comprehensive validation using multi-source remote sensing data, including evapotranspiration (ET), soil moisture (SM), and terrestrial water storage change (TWSC). The results of the comparison indicate that good overall consistency between model simulations and independent observations. Specifically, the simulated TWSC achieved an NSE of 0.66 against GRACE data, soil moisture an NSE of 0.61 against SM products, and evapotranspiration an NSE of 0.71 against the GLEAM dataset (see Supplementary Material Fig. S4-S6). Collectively, these results indicate that the coupled SRM-GSFLOW model reliably simulates surface water-groundwater interactions in the Tarim River main stem, providing a robust hydrological foundation for optimizing agricultural and ecological water use.

The variation of the surrogate model's NRMSE and R^2 with the number of training samples is shown in Supplementary Material Fig. S7. As the number of samples increases, the surrogate accuracy steadily improves. When 2842 samples are used, the coefficient of determination (R^2) reaches 0.98, corresponding to an NRMSE of 0.016.

https://doi.org/10.5194/egusphere-2026-55
Preprint. Discussion started: 15 January 2026

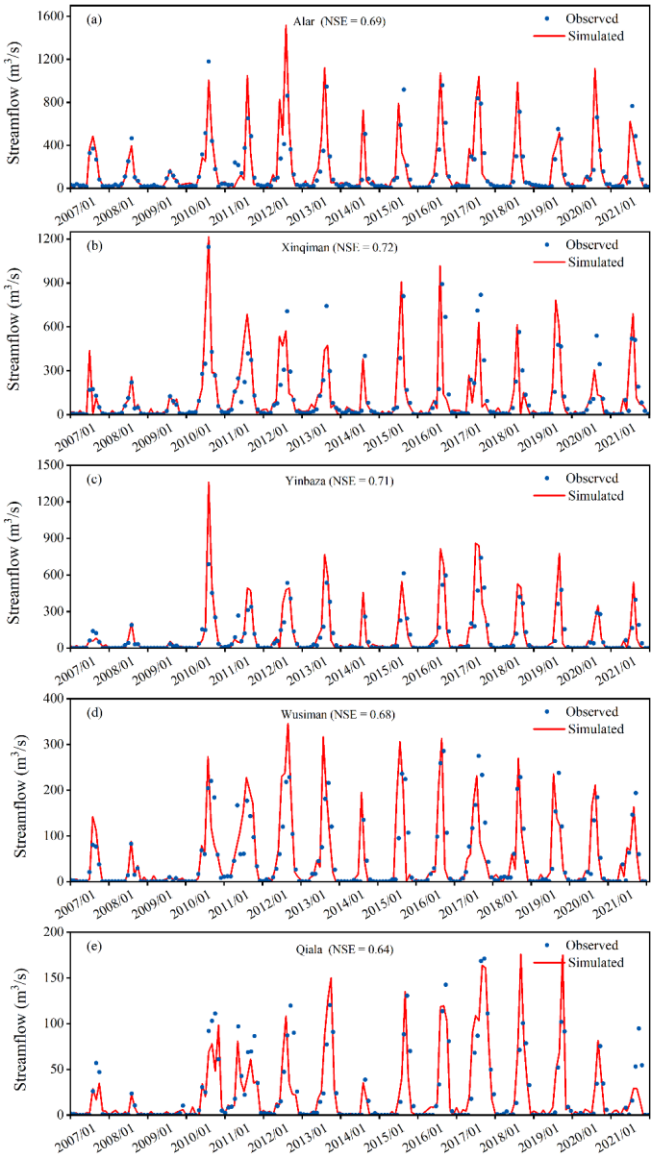

345

Figure 2. (a) - (e) present the evaluation of monthly streamflow simulations against observations at Alar and Xinqiman, Yingbaza, Wusiman, and Qiala gauging stations, respectively.

https://doi.org/10.5194/egusphere-2026-55
Preprint. Discussion started: 15 January 2026

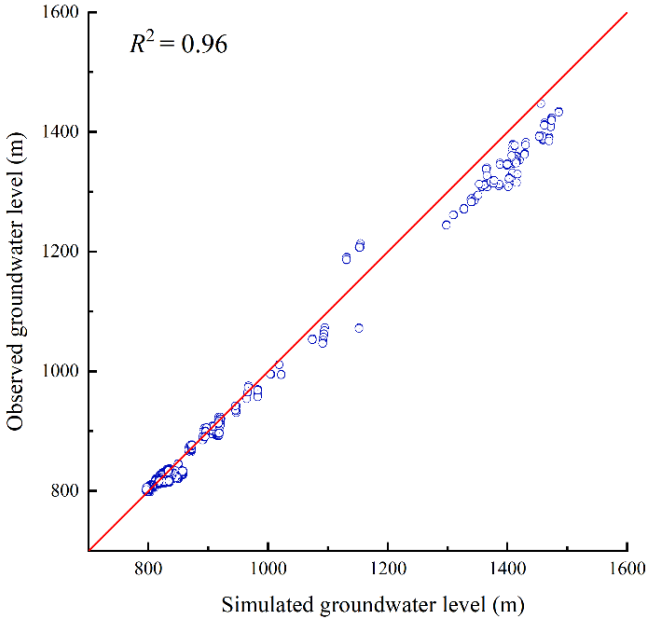

Figure 3. The evaluation of simulated groundwater levels against observations during the validation period.

4.2 Optimization Multi-objective optimization results

4.2.1 Pareto-optimal solutions

A multi-objective management model based on the NSGA-III algorithm was developed, incorporating four objective functions, namely agricultural economic benefit per unit of irrigation water (f_{AB}), average cumulative groundwater level rise (f_{GL}), surface area of Taitema Lake (f_{LA}), and total nitrogen load from agricultural non-point sources (f_{TN}).

Hydrological conditions were classified as wet, normal, or dry years based on the runoff anomaly percentage (P), as defined in Table 4. The years 2010, 2016, and 2009 were selected as representative wet, normal, and dry years, respectively.

Table 4. Annual runoff ranges under different hydrological years.

Grade	Anomaly percentage P/%	Mainstream Inflow (10^8 m^3)
High Flow Year	$P < 37.5$	$W > 63.93$
Normal Year	$37.5 < P < 87.5$	$39.53 \leqslant K \leqslant 63.93$
Low Flow Year	$P > 87.5$	$K < 39.53$

To reveal trade-offs among objectives and their variation with hydrology, parallel coordinate plots of Pareto-optimal solutions were generated for wet, normal, and dry years (Fig. 4(a)-(c)). In these plots, each objective is represented as a parallel axis, and each polyline corresponds to an optimal management strategy, illustrating interactions and trade-offs among objectives.

https://doi.org/10.5194/egusphere-2026-55
Preprint. Discussion started: 15 January 2026

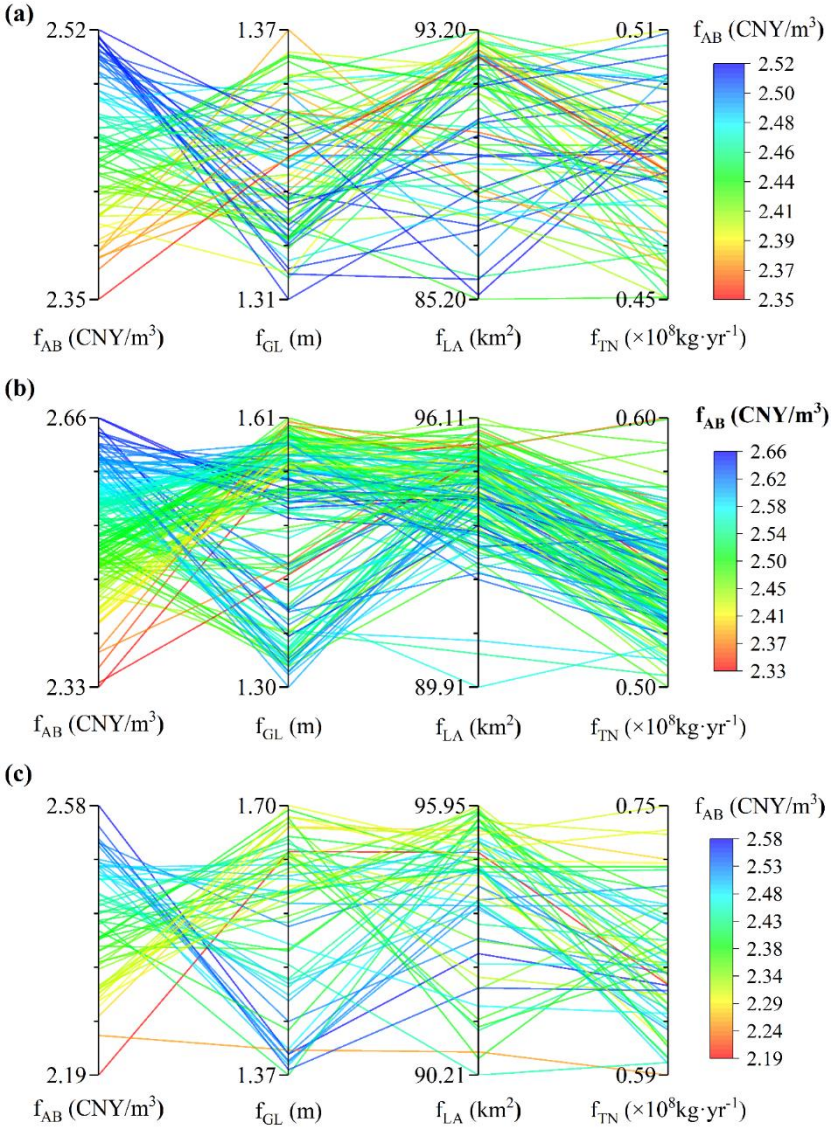

365 **Figure 4.** Objective values (y axis) plotted against management objectives f_{AB}, f_{GL}, f_{LA} and f_{TN}, with panels (a, b, c) representing dry, normal, and wet years, respectively.

The patterns in the parallel coordinate plots show an overall positive correlation between f_{AB} and f_{TN}, indicating that higher agricultural economic benefits generally coincide with increased nitrogen fertilizer use and heightened non-point source pollution. In contrast, both f_{GL} and f_{LA} exhibit negative correlations with f_{AB}. Under a fixed total surface water inflow,
370 expansion of agricultural water use tends to crowd out ecological water allocations, leading to simultaneous declines in

https://doi.org/10.5194/egusphere-2026-55
Preprint. Discussion started: 15 January 2026

groundwater recovery and terminal lake area. This highlights the inherent competition for limited water resources among agricultural production, groundwater sustainability, and terminal lake ecosystem restoration.

Across hydrological scenarios, the Pareto frontier is most expansive in wet years, indicating greater system flexibility and management space under abundant water, where conflicts among objectives are relatively weaker. In normal years, solution sets become more concentrated, reflecting a more balanced but constrained trade-off structure. In dry years, the Pareto solution space narrows substantially, and overall objective values decline, with f_{LA} decreasing by approximately 30% compared to normal years, underscoring the strong dependence of terminal lake ecological inflows on hydrological conditions.

Nonlinear trade-offs are also evident, particularly between f_{GL} and f_{AB} and between f_{GL} and f_{LA}, where the parallel coordinate plots show segments with distinct slopes. This indicates that increases in agricultural irrigation exert nonlinear impacts on groundwater levels and lake inflows, and that the multi-objective system is highly sensitive to changes in management strategies.

Overall, agricultural water use expansion enhances regional economic output but simultaneously exacerbates groundwater depletion and terminal lake degradation, reflecting the intrinsic trade-offs within the water-ecology-agriculture nexus.

4.2.2 Comparison of representative solutions and multi-objective trade-offs

To systematically evaluate trade-offs among agricultural economic benefit, groundwater security, ecological water allocation, and nitrogen pollution, five representative solutions were selected from the Pareto-optimal set under each hydrological scenario (dry, normal, and wet), resulting in a total of 15 solutions. These solutions include the solution with maximum agricultural economic benefit (S1, S6, S11), the solution with maximum groundwater level rise (S2, S7, S12), the solution with maximum terminal lake area (S3, S8, S13), the solution with minimum total nitrogen load (S4, S9, S14), and the compromise solution with the most balanced overall performance (S5, S10, S15) (Table 5). Additionally, the Pareto sets were projected onto two-dimensional planes defined by f_{AB}-f_{GL}, f_{GL}-f_{LA}, and f_{AB}-f_{TN} to illustrate synergies and conflicts among the objectives.

Figures 5-7 show Pareto-optimal solution distributions corresponding to dry, normal, and wet hydrological scenarios. Across all scenarios, a mild trade-off exists between f_{AB} and f_{GL}. High-benefit solutions (e.g., S6, S11) typically correspond to slightly lower groundwater recovery, reflecting a greater allocation of water to agriculture at the expense of ecological replenishment.

Apparently, f_{AB} shows a pronounced negative correlation with f_{LA} under all hydrological conditions. High-benefit solutions (e.g., S6, S11) typically correspond to slightly lower groundwater recovery, reflecting a greater allocation of water to agriculture at the expense of ecological replenishment. For example, in the dry year scenario, solution S1 achieves the

https://doi.org/10.5194/egusphere-2026-55
Preprint. Discussion started: 15 January 2026

highest agricultural economic benefit (2.52 CNY/m³) but results in a relatively small lake area (85.32 km²). In contrast, the ecological priority solution S3 produces a slightly lower f_{AB} (2.38 CNY/m³) while achieving the largest f_{LA} (93.20 km²). This indicates that upstream irrigation expansion directly reduces downstream ecological water availability, a pattern particularly pronounced in dry years.

Generally, f_{TN} increases with f_{AB}, although notable differences exist among individual solutions. In the wet year scenario, the compromise solution S15 yields a f_{AB} of 2.32 CNY/m³ with a corresponding f_{TN} of 0.66×10^8 kg/yr, which is lower than that of the high-output solution S11 (f_{AB} = 2.58 CNY/m³, f_{TN} = 0.74×10^8 kg/yr) and the low-nitrogen solution S14 (f_{AB} = 2.31 CNY/m³, f_{TN} = 0.69×10^8 kg/yr). This suggests that even when prioritizing economic output, non-point source pollution can be mitigated through appropriate management. Nevertheless, the overall trend confirms that higher agricultural benefits generally rely on greater fertilizer inputs, highlighting a persistent conflict between production and environmental protection. This conflict necessitates coordinated management through precision fertilization and optimized crop structure.

Comparing the compromise solutions (S5, S10, S15) across scenarios further reveals their scenario-dependent nature. In the dry year (S5), moderate agricultural benefits (2.43 CNY/m³) are achieved alongside relatively high ecological water supply (90.88 km²) and low nitrogen load (0.47×10^8 kg/yr). In the normal year (S10), a more balanced combination of economic and ecological benefits is obtained (f_{AB} = 2.44 CNY/m³, f_{LA} = 93.57 km²), while maintaining a low nitrogen load (0.54×10^8 kg/yr). In the wet year (S15), f_{AB} (2.32 CNY/m³) remains at an intermediate level, with f_{LA} (90.71 km²) and f_{GL} (1.46 m) also showing moderate performance, and f_{TN} (0.66×10^8 kg/yr) remaining lower than that of high-output solutions. These results reflect a clear compromise, rather than the comprehensive optimization of any single objective.

Overall, compromise solutions achieve relatively balanced performance across conflicting objectives, but this balance comes at the cost of sacrificing optimal performance in any single objective. Comparisons across hydrological scenarios show that management flexibility is greatest in wet years, while multi-objective conflicts intensify during dry years, when trade-offs between agricultural expansion and ecological water requirements become particularly pronounced.

https://doi.org/10.5194/egusphere-2026-55
Preprint. Discussion started: 15 January 2026

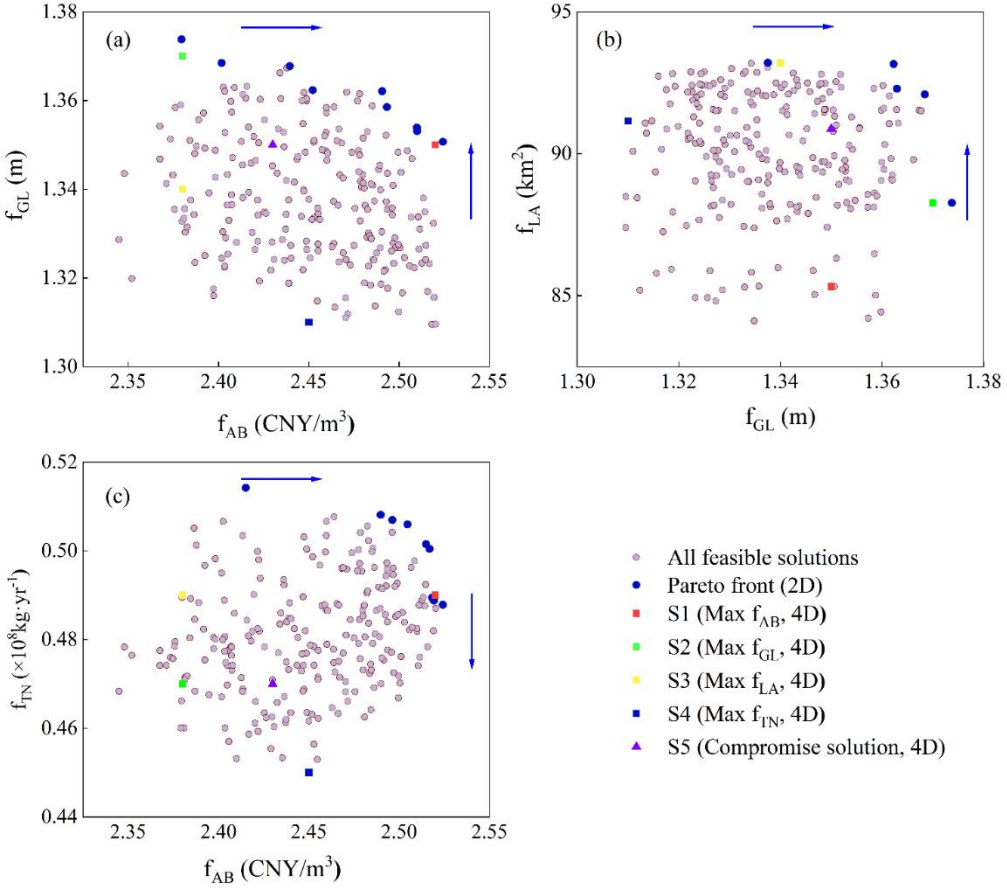

Figure 5. Scatter plots for optimization in a dry year exhibiting the correlation between each pair of objectives, (a) f_{AB} and f_{GL}; (b) f_{GL} and f_{LA}; and (c) f_{AB} and f_{TN}. Each dot represents a feasible solution. The representative solutions for dry scenario (S1-S5) can be identified by rectangles with different color. The navy-blue arrow indicates the direction of Pareto optimality.

https://doi.org/10.5194/egusphere-2026-55
Preprint. Discussion started: 15 January 2026

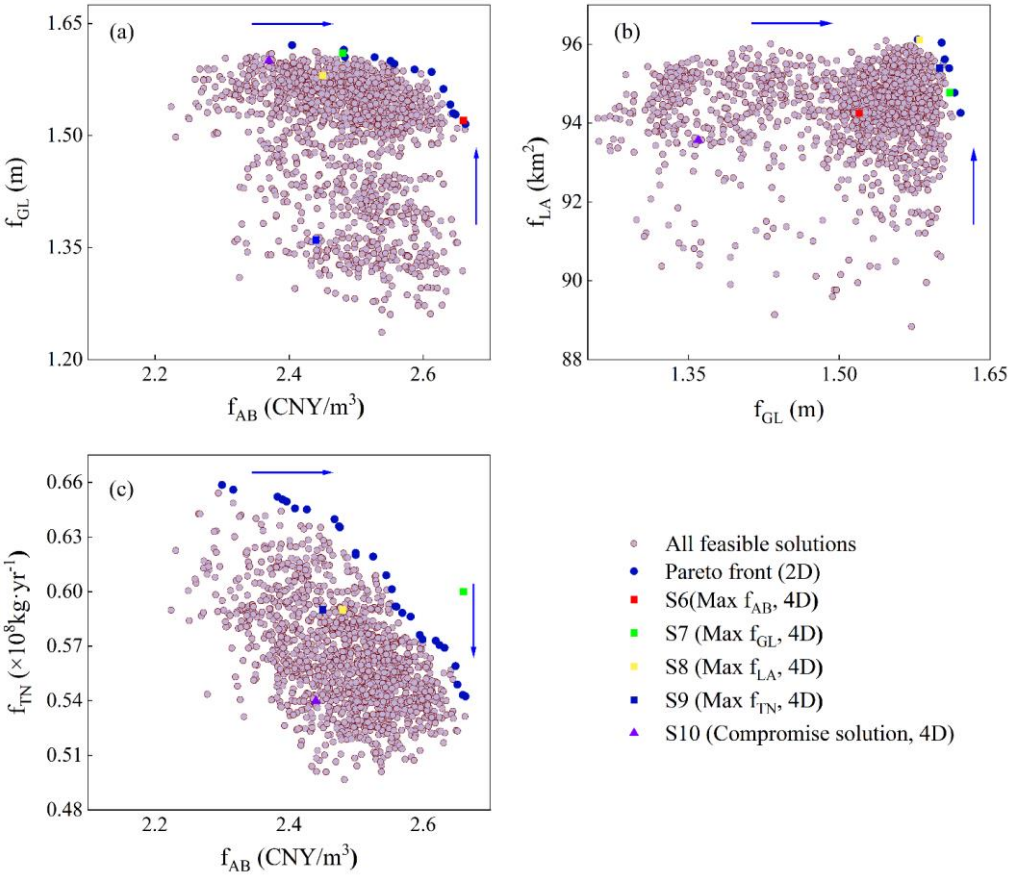

Figure 6. Scatter diagrams depicting correlations among objective pairs in a normal year, (a) f_{AB} and f_{GL}; (b) f_{GL} and f_{LA}; and (c) f_{AB} and f_{TN}. Representative normal-year solutions (S6-S10) are marked using colored rectangles.

https://doi.org/10.5194/egusphere-2026-55
Preprint. Discussion started: 15 January 2026

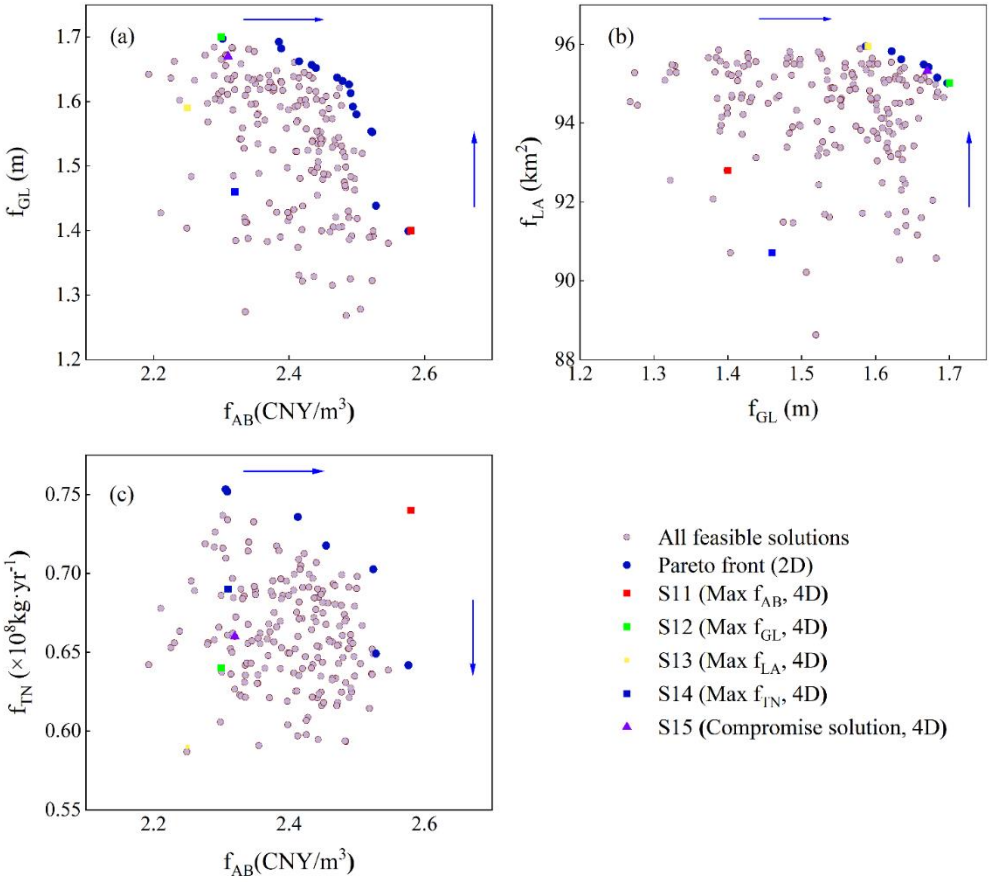

Figure 7. Scatter diagrams depicting correlations among objective pairs under a wet year, (a) f_{AB} and f_{GL}; (b) f_{GL} and f_{LA}; and (c) f_{AB} and f_{TN}. Representative wet-year solutions (S11-S15) are marked using colored rectangles.

435

440

https://doi.org/10.5194/egusphere-2026-55
Preprint. Discussion started: 15 January 2026

Table 5. Objective values for each of the 15 solutions.

Scenario	Solutions	f_{AB} (CNY/m^3)	f_{GL} (m)	f_{LA} (km^2)	f_{TN} (×10^8 kg/yr)
	S1	2.52	1.35	85.32	0.49
	S2	2.38	1.37	88.27	0.47
Dry	S3	2.38	1.34	93.20	0.49
	S4	2.45	1.31	91.15	0.45
	S5	2.43	1.35	90.88	0.47
	S6	2.66	1.52	94.25	0.60
	S7	2.48	1.61	94.77	0.59
Normal	S8	2.45	1.58	96.11	0.58
	S9	2.37	1.60	95.39	0.51
	S10	2.44	1.36	93.57	0.54
	S11	2.58	1.40	92.80	0.74
	S12	2.30	1.70	95.01	0.64
Wet	S13	2.25	1.59	95.95	0.59
	S14	2.31	1.67	95.32	0.69
	S15	2.32	1.46	90.71	0.66

4.2.3 Suitable cultivated land area

Table 6 presents the suitable cultivated land area ranges and corresponding optimal cropping structures under different hydrological scenarios. Suitable cultivation scale varies substantially across hydrological conditions. The suitable cultivated area ranges from 11.3×10⁴-14.3×10⁴ hm² in wet years, declines to 10.1×10⁴-13.1×10⁴ hm² in normal years, and contracts further to 9.5×10⁴-11.9×10⁴ hm² in dry years. These results demonstrate that available water is the primary constraint on regional agricultural scale.

Table 6. Optimal crop structure proportions and suitable cultivated land area under different hydrological scenarios.

Hydrological Year	Suitable Cultivated Area (10⁴ hm²)	Maize	Cotton	Vegetables	Melons	Oilseed	Fruits
Low Flow Year	9.5-11.9	2.84	75.84	1.71	1.71	2.72	9.2
Normal Year	10.1-13.1	4.68	69.83	2.48	2.69	3.25	11.23
High Flow Year	11.3-14.3	6.58	69.72	4.82	2.43	4.15	7.56

Comparing optimal cropping structures across scenarios reveals that improved water availability favors allocating land to high-benefit crops. The proportions of vegetables and melons increase steadily, rising by 3.11% and 0.72%, respectively, in wet versus dry years, whereas those of maize and oil crops decline. The proportion of fruit crops decreases to 7.56% in wet years (down 1.64% from dry years), reflecting their heightened sensitivity to ecological and water quality constraints in multi-objective trade-offs. Overall, the optimized cropping structures achieve a coordinated balance between cultivated land scale and water resource utilization through adjustments in crop composition.

https://doi.org/10.5194/egusphere-2026-55
Preprint. Discussion started: 15 January 2026

Figures 8a-c show the spatial distribution of suitable cultivated land area across the study regions under dry, normal, and wet hydrological scenarios. Under dry conditions (Fig. 8(a)), cultivated land area shows pronounced spatial heterogeneity. In the upstream area, Zone 1 has the most stable cultivated area (3.30-4.30×10⁴ hm²), significantly larger than that of the most water-constrained Zone 4 (approximately 0.26-0.39×10⁴ hm²). In the midstream, Zones 5 and 6 show the widest fluctuation ranges, indicating high sensitivity to trade-offs. In the downstream area, Zone 7 shows a marked contraction in scenarios prioritizing ecological objectives.

Under normal conditions (Fig. 8(b)), cultivated land area increases in all regions relative to dry years. In the upstream area, Zone 3 exhibits substantial variability (1.09×10⁴-1.83×10⁴hm²), indicating that its cultivated area is strongly co-determined by crop structure adjustments and water availability. In the midstream area, Zone 6 expands notably, whereas downstream Zone 7 remains tightly constrained by ecological water demands.

Under wet conditions (Fig. 8(c)), the land's carrying capacity for agriculture increases markedly. The downstream Zone 7 responds most strongly, reaching 3.84×10⁴ hm² in solution S12, indicating substantial expansion potential. However, the upstream Zone 3 shows contraction under ecology-oriented or water-quality-oriented solutions, indicating that ecological objectives remain binding constraints even under abundant water conditions.

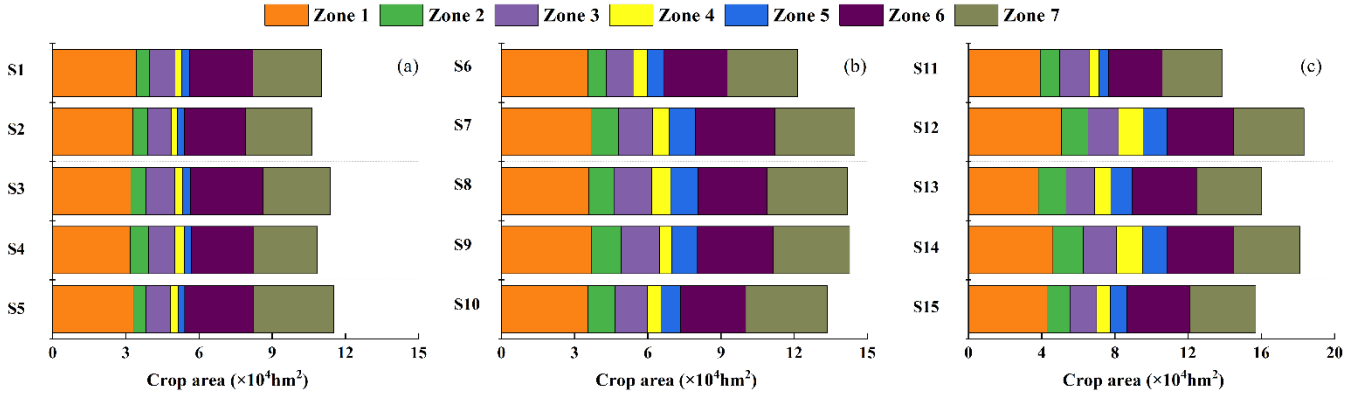

Figure 8. Suitable cultivated land area in each region under different hydrological scenarios.

Overall, regional variation in suitable cultivated area is jointly shaped by hydrological conditions and management preferences. Cultivated area must contract during dry years but can expand in wet years. The midstream area is most sensitive to trade-offs, while the downstream area has the greatest expansion potential in wet years. These findings confirm that hydrological conditions dominate agricultural scale regulation, and that multi-objective optimization offers feasible pathways to balance economic and ecological objectives.

https://doi.org/10.5194/egusphere-2026-55
Preprint. Discussion started: 15 January 2026

4.2.4 Crop structure optimization based on multi-objective trade-offs

Based on the identified suitable land scales, this section examines how optimal cropping structures adjust to different hydrological conditions. Figure 9 presents the optimal cropping structures corresponding to solutions S1-S15.

As total irrigation demand rises from 110.75 to 136.98×10⁸ m³ from dry to wet years, cropping structures adjust systematically. High-benefit crops expand continuously, with the proportion of vegetables increasing by 3.11% and that of melons rising slightly by 0.72%, while the proportion of fruit crops decreases by 1.64%. This pattern indicates that, under multi-objective constraints, crop allocation increasingly emphasizes integrated economic and environmental performance. In contrast, maize and oil crop proportions rise slightly in wet years, suggesting they retain a competitive advantage when water is plentiful.

In dry years (S1-S5), the proportions of cotton and vegetables decline markedly across all regions, while maize and oil crops account for a relatively larger share. In Zones 4-7, the cultivated area of water-intensive melon crops is substantially restricted to reduce pressures on downstream ecological water demands.

Ecological protection objectives are a key constraint on cropping structure. In dry years, water-intensive melon cultivation in the midstream and downstream regions (Zones 4-7) is strictly limited to safeguard downstream ecological baseflows. Even in wet years with relatively abundant water, the expansion of water-intensive melons and fruit trees in downstream Zones 6-7 remains limited to avoid excessive irrigation demand during critical ecological windows, such as the germination of Populus euphratica forests.

As shown in Table 7, total nitrogen input increases from 4.71×10⁴ t in dry years to 5.87×10⁴ t in wet years, broadly tracking the expansion of cultivated land area and without pronounced spatial concentration. This indicates that the optimized cropping structures achieve a relatively even distribution of nitrogen fertilizer inputs, effectively avoiding localized intensification of environmental risks.

In summary, the optimal cropping structure is a dynamic system that flexibly adjusts crop composition to hydrological variability while respecting ecological thresholds.

Table 7. Agricultural area, water demand, and nitrogen input under representative scenarios.

Hydrological Year	Total Cultivated Area (10^4 hm²)	Total Water Demand (10^8m³)	Total Nitrogen Input (10^3 t)
Low Flow Year (S5)	11.02	110.75	4.71
Normal Year (S10)	12.14	121.21	5.19
High Flow Year (S15)	13.85	136.98	5.87

https://doi.org/10.5194/egusphere-2026-55
Preprint. Discussion started: 15 January 2026

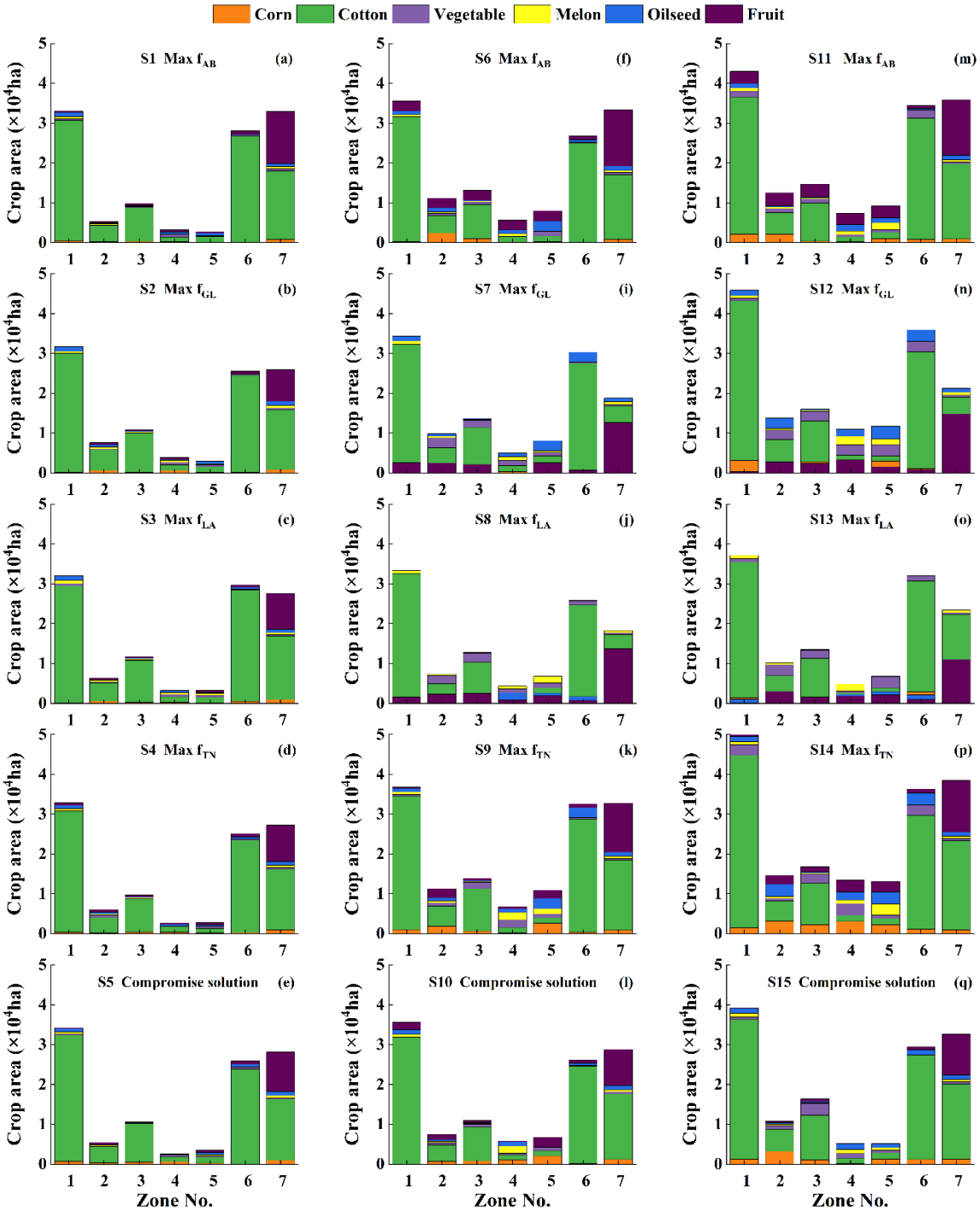

Figure 9. Crop planting structures (corn, cotton, vegetable, melon, oilseed and fruit) for the selected solutions (S1-S15), with panels (a)-(e), (f)-(l), (i)-(q) representing wet, normal, and dry years, respectively.

https://doi.org/10.5194/egusphere-2026-55
Preprint. Discussion started: 15 January 2026

5. Discussion

5.1 Implications for coordinated water-agriculture-ecosystem management in arid river basins

This study develops a multi-objective water-agriculture-ecosystem (WAE) optimization framework to systematically elucidate the coordination between cropping structure adjustment and water allocation in the Tarim River mainstream. The results reveal pronounced trade-offs between agricultural economic benefits (f_{AB}) and ecological objectives (f_{LA} and f_{GL}), as well as environmental objectives (f_{TN}), confirming the widely recognized "water-food-ecosystem" dilemma in arid inland river basins (Liu et al., 2017). Compared with the ecological crises driven by upstream-downstream water competition in the Aral Sea Basin (Azimov et al., 2022), the multi-objective optimization approach adopted here provides a quantitative tool to explicitly characterize and manage such conflicts.

Notably, conflicts between f_{AB} and ecological objectives (f_{GL}, f_{LA}) can be mitigated through scientifically designed adjustments to cropping structure and irrigation practices. This suggests that sustaining agricultural output can be compatible with ecological preservation, providing fresh perspectives for managing water resources in arid regions.

Hydrological conditions strongly regulate system-level trade-offs. During dry years, system resilience declines markedly and multi-objective conflicts intensify, consistent with observations from the Aral Sea Basin where upstream-downstream tensions are exacerbated under drought conditions (Saidmamatov et al., 2020). In contrast, wet years provide greater management flexibility and create critical windows of opportunity for achieving multi-objective coordination through structural adjustment rather than rigid water allocation constraints.

The compromise solutions identified in this study exhibit robust overall performance across different hydrological scenarios. Hydrological conditions strongly regulate system-level trade-offs. Their strength lies in shifting the paradigm from a "win-lose" trade-off toward a more balanced "shared-benefit" outcome. For example, under dry-year conditions, solution S5 maintains moderate agricultural economic returns while effectively safeguarding ecological water requirements and controlling nitrogen pollution risks. This structurally optimized pathway aligns with recent practical efforts in the adjacent Yanqi Basin, where cropping structure adjustment has been used to achieve simultaneous economic and ecological gains (Tang et al., 2024). The present study further strengthens such empirical findings by providing quantitative, system-level evidence.

Spatial heterogeneity analysis underscores the necessity of differentiated management strategies. The midstream area exhibits the highest sensitivity to multi-objective trade-offs and thus requires more refined water-use regulation. Although the downstream area shows expansion potential during wet years, strict adherence to ecological thresholds remains essential. These findings are highly consistent with the differentiated management principles embodied in Xinjiang's "Three Red Lines" water policy (Taon et al., 2012).

https://doi.org/10.5194/egusphere-2026-55
Preprint. Discussion started: 15 January 2026

Dynamically optimizing cropping structure is a key pathway to multi-objective coordination. As hydrological conditions improve, the proportion of high-benefit crops can be moderately increased, but such adjustments must remain firmly constrained by ecological safety considerations. In downstream ecologically sensitive zones, even under relatively abundant water availability, the expansion of high water-consuming crops should be strictly limited. This "ecology-first" optimization principle is critical for maintaining long-term ecological security in arid river basins.

5.2 Limitations of the study

Although the proposed framework offers a theoretical foundation and a decision-support tool for integrated WAE management in arid areas, several limitations should be recognized.

First, the practical feasibility of the optimized solutions requires further field validation. Owing to the lack of long-term, large-scale monitoring data that simultaneously capture cropping structure adjustment and ecological water conveyance processes, the real-world applicability of the identified Pareto-optimal solutions remains uncertain. Future research should integrate data from ecological water regulation projects and water-saving agriculture demonstration programs to further calibrate and validate model outputs.

Second, scale transformation during model construction may introduce uncertainty. This study couples basin-scale hydrological simulations with grid-based land use and crop distribution data, and errors arising from spatial scaling and parameter aggregation are difficult to fully quantify. In addition, the influence of future climate change on runoff patterns and crop water requirements has not been explicitly addressed. Including climate change scenarios constitutes a key avenue for future studies.

Finally, environmental impact assessment remains simplified. The estimation of agricultural non-point source pollution relies on generalized parameterization, with limited representation of spatial heterogeneity in soil properties, fertilization practices, and pollutant transport processes. Similarly, ecological water demand is primarily defined based on historical hydrological conditions, without fully accounting for dynamic ecosystem responses of natural vegetation. The application of higher-resolution process-based models could further enhance the precision and reliability of system simulations.

6. Conclusions

A coordinated water-ecosystem-agriculture (WEA) management framework is critical for alleviating conflicts between ecological degradation and agricultural development in arid inland river basins. Focusing on the mainstream region of the Tarim River Basin as a case study, this research constructs a coupled hydrology-agriculture multi-objective optimization model to systematically characterize trade-offs among multiple objectives and to propose strategies for coordinated WEA management. The main conclusions are summarized as follows.

Multi-objective optimization demonstrates pervasive trade-offs within the WEA system. Significant trade-offs are observed among agricultural economic benefit (f_{AB}), terminal lake area (f_{LA}), and total nitrogen load (f_{TN}). Solutions that

https://doi.org/10.5194/egusphere-2026-55
Preprint. Discussion started: 15 January 2026

maximize economic output achieve higher agricultural returns at the cost of reduced ecological water availability and increased nitrogen pollution, whereas solutions emphasizing ecological or environmental objectives require moderate reductions in agricultural output. These results indicate that strategies solely focused on agricultural expansion are unsustainable and underscore the need for systematic balancing of multiple objectives.

Spatially differentiated regulation based on regional heterogeneity effectively balances water, ecological, and agricultural objectives. Upstream irrigation districts, benefiting from relatively stable water availability, maintain higher levels of agricultural production under multi-objective trade-offs. By contrast, midstream and downstream areas are highly sensitive to ecological water level and conveyance constraints, resulting in larger fluctuations in agricultural scale and stricter restrictions on the expansion of water-intensive crops. These results underscore the need for management strategies tailored to the specific conditions of arid river basins.

Under multi-objective optimization, cropping structures can be dynamically adjusted to coordinate cultivated land scale and crop composition. Cotton consistently dominates the optimized cropping structure (69.72%-75.84%), providing stability to regional agricultural economic performance. Cropping structures respond dynamically to hydrological conditions. During wet years, the cultivated land area can be moderately expanded to 11.3×10^4-14.3×10^4 hm^2, with greater allocation to high-value crops, including vegetables. In contrast, during dry years, cultivated land must be reduced to 9.5×10^4-11.9×10^4 hm^2, placing more emphasis on water-saving crops such as maize and oil crops, while strictly limiting the planting of high water-consuming crops in midstream and downstream areas. This optimized configuration ensures coordinated management of cultivated land scale, crop structure, and nitrogen inputs, thereby preventing localized intensification of environmental risks.

Author contributions.

Conceptualization, X.Z.; data collection, D.C; methodology, D.C. and X.Z.; validation, D.C. and X.Z.; writing-original draft preparation, D.C.; writing-review and editing, D.C. and X.Z.; supervision, D.G., D.W. and J.W.; project administration, D.G., D.W. and J.W.. All authors have read and agreed to the published version of the manuscript.

Competing interests.

On behalf of all authors, the corresponding author states that there are no conflicts of interest.

Data Availability.

The ERA5 reanalysis precipitation data (Hersbach et al., 2020) can be downloaded from https://cds.climate.copernicus.eu/cdsapp#!/dataset/reanalysis-era5-land?tab=form. The GLEAM_v3.5a data (Martens et al., 2017; Miralles et al., 2011) is available at https://www.gleam.eu/. The GRACE RL06 Center for Space Research (CSR) mascon products (Save et al., 2016) can be acquired from https://www2.csr.utexas.edu/grace/RL06_mascons.html. Monthly streamflow data simulated by the SRM model have been made publicly available via the zenodo platform (https://doi.org/10.5281/zenodo.18151460, Zeng and Chen., 2025).

https://doi.org/10.5194/egusphere-2026-55
Preprint. Discussion started: 15 January 2026

Acknowledgements.

The authors want to thank the High-Performance Computing Center (HPCC) of Nanjing University for performing the simulations in this paper.

Financial support.

This study was supported by the National Natural Science Foundation of China (42477082).

References

Avellán, T., Ardakanian, R., Perret, S. R., Ragab, R., Vlotman, W., Zainal, H., Im, S., and Gany, H. A.: Considering resources beyond water: irrigation and drainage management in the context of the water-energy-food nexus, Irrig. Drain., 67, 12-21, https://doi.org/10.1002/ird.2154, 2018.

Azimov, U., Avezova, N.: Sustainable small-scale hydropower solutions in central Asian countries for local and cross-border energy/water supply. Renew. Sustain. Energy Rev. 167, 112726. https://doi.org/10.1016/j.rser.2022.112726, 2022.

Beaudoing, H. and Rodell, M.: NASA GLDAS-2.1 Noah Land Surface Model for 2002-2021, NASA Goddard Earth Sciences Data and Information Services Center [data set], https://doi.org/10.5067/SXAVCZFAQLNO, 2020.

Brown, R. J. E.: Permafrost in Canada, Geol. Surv. of Can., Ottawa, Ont., Map 1246A, 1967.

Campbell, B. M., Beare, D. J., Bennett, E. M., Hall-Spencer, J. M., Ingram, J. S. I., Jaramillo, F., Ortiz, R., Ramankutty, N., Sayer, J. A., and Shindell, D.: Agriculture production as a major driver of the Earth system exceeding planetary boundaries, Ecol. Soc., 22, 8, https://doi.org/10.5751/ES-09595-220408, 2017.

Cao, Z., Zhu, T., and Cai, X.: Hydro-agro-economic optimization for irrigated farming in an arid region: the Hetao Irrigation District, Inner Mongolia, Agric. Water Manag., 277, 108095, https://doi.org/10.1016/j.agwat.2022.108095, 2023.

Cosgrove, W. J. and Loucks, D. P.: Water management: current and future challenges and research directions, Water Resour. Res., 51, 4823-4839, https://doi.org/10.1002/2014WR016869, 2015.

CSR (Center for Space Research): GRACE terrestrial water storage anomalies, University of Texas at Austin [data set], https://doi.org/10.5067/TEMSC-3JC63, 2023.

Falkenmark, M. and Lannerstad, M.: Consumptive water use to feed humanity - curing a blind spot, Hydrol. Earth Syst. Sci., 9, 15-28, https://doi.org/10.5194/hess-9-15-2005, 2005.

Flörke, M., Schneider, C., and McDonald, R. I.: Water competition between cities and agriculture driven by climate change and urban growth, Nat. Sustain., 1, 51-58, https://doi.org/10.1038/s41893-017-0006-8, 2018.

Gong, P., Wang, J., Yu, L., Zhao, Y., Liang, L., Niu, Z., Huang, X., Fu, H., Liu, S., Li, C., Li, X., Fu, W., Liu, C., Xu, Y., Wang, X., Cheng, Q., Hu, L., Yao, W., Zhang, H., Zhu, P., Zhao, Z., Zhang, H., Zheng, Y., Ji, L., Zhang, Y., Chen, H.,

https://doi.org/10.5194/egusphere-2026-55
Preprint. Discussion started: 15 January 2026

Yan, A., Guo, J., Yu, L., Wang, L., Liu, X., Shi, T., Zhu, M., Chen, Y., Yang, G., Tang, P., Xu, B., Giri, C., Clinton, N., Zhu, Z., Chen, J., and Chen, J.: Finer resolution observation and monitoring of global land cover: first mapping results with Landsat TM and ETM+ data, Int. J. Remote Sens., 34, 2607-2654, https://doi.org/10.1080/01431161.2012.748992, 2013.

Gordon, L. J., Finlayson, C. M., and Falkenmark, M.: Managing water in agriculture for food production and other ecosystem services, Agric. Water Manag., 97, 512-519, https://doi.org/10.1016/j.agwat.2009.03.017, 2010.

Hersbach, H., Bell, B., Berrisford, P., Hirahara, S., Horányi, A., Muñoz-Sabater, J., et al.: The ERA5 global reanalysis, Q. J. R. Meteorol. Soc., 146, 1999-2049, https://doi.org/10.1002/qj.3803, 2020.

IPCC: Summary for policymakers, in: Climate Change 2022: Impacts, Adaptation and Vulnerability, Cambridge University Press, https://doi.org/10.1017/9781009157940.001, 2022.

Jalilov, S., Amer, S. A., and Ward, F. A.: Managing the water-energy-food nexus: opportunities in Central Asia, J. Hydrol., 557, 407-425, https://doi.org/10.1016/j.jhydrol.2017.12.040, 2018.

Karner, K., Schmid, E., Schneider, U. A., and Mitter, H.: Computing stochastic Pareto frontiers between economic and environmental goals for a semi-arid agricultural production region in Austria, Ecol. Econ., 185, 107044, https://doi.org/10.1016/j.ecolecon.2021.107044, 2021.

Li, Z., Zhang, Y., Liu, X., Zhang, W., and Tao, F.: Vegetation distribution map of China (1:1,000,000), National Tibetan Plateau Data Center [data set], https://doi.org/10.11888/VegetationMap.tpdc.270910, 2017.

Mao, J., Shi, X., Thornton, P. E., Piao, S., and Wang, X.: Soil moisture in China dataset (2000-2019), National Tibetan Plateau Data Center [data set], https://doi.org/10.11888/Soil.tpdc.270912, 2021.

Martens, B., Miralles, D. G., Lievens, H., van der Schalie, R., de Jeu, R. A. M., Fernández-Prieto, D., Beck, H. E., Dorigo, W. A., and Verhoest, N. E. C.: GLEAM v3: Satellite-based land evaporation and root-zone soil moisture, Geosci. Model Dev., 10, 1903-1925, https://doi.org/10.5194/gmd-10-1903-2017, 2017.

Meng, X., Mao, J., Shi, X., and Piao, S.: Soil moisture in China dataset supplement (2020-2021), National Tibetan Plateau Data Center [data set], https://doi.org/10.11888/Soil.tpdc.270913, 2021.

Ministry of Agriculture and Rural Affairs of Xinjiang, 2002-2025: National Agricultural Product Cost-Benefit Compilation and Annual Crop Price Statistics. Urumqi: Ministry of Agriculture and Rural Affairs of Xinjiang. [Online] Available at: https://nynct.xinjiang.gov.cn/ (accessed 6 November 2025).

Monger, J. W. H. and Journeay, J. M.: Guide to the geology and tectonic evolution of the southern Coast Mountains, Geol. Surv. of Can., Ottawa, Ont., Open File Rep. 2490, 77 pp., 1994.

https://doi.org/10.5194/egusphere-2026-55
Preprint. Discussion started: 15 January 2026

Naranjo, L., Correa-Cano, M. E., Rey, D., Chengot, R., España, F., Sactic, M., Knox, J. W., Yan, X., Viteri-Salazar, O., Foster, W., and Melo, O.: A scenario-specific nexus modelling toolkit to identify trade-offs in the promotion of sustainable irrigated agriculture in Ecuador, a Belt and Road country, J. Clean. Prod., 413, 137350, https://doi.org/10.1016/j.jclepro.2023.137350, 2023.

National Bureau of Statistics of China, 2002-2021: China Statistical Yearbook. Beijing: National Bureau of Statistics of China. [Online] Available at: https://www.stats.gov.cn/ (accessed 6 November 2025).

Niu, G., Zheng, Y., Han, F., and Qin, H.: The nexus of water, ecosystems and agriculture in arid areas: a multi-objective optimization study on system efficiencies, Agric. Water Manag., 223, 105697, https://doi.org/10.1016/j.agwat.2019.105697, 2019.

Rodell, M., Houser, P. R., Jambor, U., Gottschalck, J., Mitchell, K., Meng, C. J., Arsenault, K., Cosgrove, B., Radakovich, J., Bosilovich, M., Entin, J. K., Walker, J. P., Lohmann, D., and Toll, D.: The Global Land Data Assimilation System, Bull. Am. Meteorol. Soc., 85, 381-394, https://doi.org/10.1175/BAMS-85-3-381, 2004.

Saidmamatov, Olimjon, Inna Rudenko, Stephan Pfister, and Jacek Koziel.: "Water-Energy-Food Nexus Framework for Promoting Regional Integration in Central Asia" Water 12, no. 7: 1896. https://doi.org/10.3390/w12071896, 2020

Song, J., Yang, Y., Sun, X., Lin, J., Wu, M., Wu, J., and Wu, J.: Basin-scale multi-objective simulation-optimization modeling for conjunctive use of surface water and groundwater in northwest China, Hydrol. Earth Syst. Sci., 24, 2323-2341, https://doi.org/10.5194/hess-24-2323-2020, 2020.

Qiu, Y., Wang, X. (2020). High Asia Daily Snow Cover Fraction Dataset (2002-2018). The dataset is provided by National Cryosphere Desert Data Center (http://www.ncdc.ac.cn). https://cstr.cn/11738.11.ncdc.nieer.2020.1660. https://doi.org/10.11922/sciencedb.457.

Tang, X., Huang, Y., Pan, X., Liu, T., Ling, Y., and Peng, J.: Managing the water-agriculture-environment-energy nexus: trade-offs and synergies in an arid area of Northwest China, Agric. Water Manag., 295, 108776, https://doi.org/10.1016/j.agwat.2024.108776, 2024.

Tao, J., Zuo, Q.T., Xue, H.L., Dou, M., Liang, S.K., and Mao, C.C.: Control Indicators and Determination Methods of "Three Red Lines" of the Strictest Water Resources Management System, Water Saving Irrigation, (04), 64-67, https://kns.cnki.net/kcms2/article/abstract?v=OfZxIIxxsvAY5sydd0hGq84pIosExzfH938SRuOOFQ4UDwZy-7MHrI5ycHZmtn8GKy2o1hF7E8HQk77_n_gseSF21ImzKtqmO9PyWMjqm84GUe1NUm9siR6jrRkU6JkL14NBbZlEIfDvZ81dlqce_7wkEvOZiaPp6zB_98Q0Pv2R7rW4NF4uZA==&uniplatform=NZKPT&language=CHS, 2012.

Wang, G., Xu, S., and Xie, Z.: Study on suitable lake area of Taitema Lake, Groundwater, 41, 6-10, https://doi.org/10.16616/j.cnki.11-4446/TV.2021.09.02, 2021.

https://doi.org/10.5194/egusphere-2026-55
Preprint. Discussion started: 15 January 2026

Wang, Y., Chen, M., Yan, L., Yang, G., Ma, J., and Deng, W.: Quantifying threshold water tables for ecological restoration in arid northwestern China, Groundwater, 58, 132-142, https://doi.org/10.1111/gwat.12934, 2020.

Wang, Y., Guo, X., Zhang, F., Yin, H., Guo, P., Zhang, W., and Li, Q.: The spatially-distributed ANN-optimization approach for water-agriculture-ecology nexus management under uncertainties and risks, Agric. Water Manag., 271, 107780, https://doi.org/10.1016/j.agwat.2022.107780, 2022.

Watson, J. E. M., Iwamura, T., and Butt, N.: Mapping vulnerability and conservation adaptation strategies under climate change, Nat. Clim. Chang., 3, 989-994, https://doi.org/10.1038/nclimate2007, 2013.

Wieder, W. R., Boehnert, J., Bonan, G. B., and Langseth, M.: Harmonized World Soil Database (version 1.2), ORNL DAAC [data set], https://doi.org/10.3334/ORNLDAAC/1247, 2014.

Xinjiang Water Resources Department, 2002-2021: Xinjiang Water Resources Bulletin. Urumqi: Xinjiang Water Resources Department. [Online] Available at: https://slt.xinjiang.gov.cn/ (accessed 6 November 2025).

Ye, Z., Chen, S., Zhang, Q., Liu, Y., and Zhou, H.: Ecological water demand of Taitema Lake in the lower reaches of the Tarim River and the Cherchen River, Remote Sens., 14, 832, https://doi.org/10.3390/rs14040832, 2022.

Yin, Z., Wu, J., Song, J., Yang, Y., Zhu, X., and Wu, J.: Multi-objective optimization-based reactive nitrogen transport modeling for the water-environment-agriculture nexus in a basin-scale coastal aquifer, Water Res., 212, 118111, https://doi.org/10.1016/j.watres.2022.118111, 2022.

Zhang, X. and Ren, L.: Simulating and assessing the effects of seasonal fallow schemes on the water-food-energy nexus in a shallow groundwater-fed plain of the Haihe River basin of China, J. Hydrol., 595, 125992, https://doi.org/10.1016/j.jhydrol.2021.125992, 2021.

Zeng, X. and Chen, D.: A coupled surface water-groundwater multi-objective optimization framework for coordinated water-ecosystem-agriculture management in arid inland river basin, Zenodo, [data set], https://doi.org/10.5281/zenodo.18151460, 2025.

Zhong, L., Gong, P., Ma, R., and Mu, Q.: Reconstructed terrestrial water storage dataset (2002-2019), National Tibetan Plateau Data Center [data set], https://doi.org/10.11888/Hydro.tpdc.270990, 2020.

Zhong, L., Ma, R., Gong, P., and Mu, Q.: Reconstructed terrestrial water storage dataset supplement (2017-2019), National Tibetan Plateau Data Center [data set], https://doi.org/10.11888/Hydro.tpdc.270911, 2020.

Zhu, X.: Study on multi-objective water resources allocation scheme in the lower reaches of the Tarim River, Groundwater, 44, 213-215, https://doi.org/10.19807/j.cnki.DXS.2022-02-073, 2022.